Multi-Pulse Processing Algorithm for Improving Mean Velocity Estimation in Weather Radar

Juan P. Pascual, Jorge Cogo, Arturo Collado Rosell and Javier Areta, *Member, IEEE*

***Abstract*—In this paper we present a novel algorithm termed *Multi-Pulse Processing* (MPP) for improving mean Doppler velocity estimation in weather radar applications. It can be used for both staggered pulse repetition time (PRT) and uniform-PRT sequences. Essentially, MPP consists of finding a particular zero of a functional composed of data autocorrelation estimates at multiple lags. To select the proper zero an initial Doppler velocity estimate is required. Therefore, MPP can be considered as an estimation refinement stage. Its advantage lies in the fact that it uses the complete information contained in the radar signal autocorrelation. After a theoretical analysis, we compare the performance of MPP against other well-established methods of similar complexity and the Cramér-Rao lower bound, by means of Monte-Carlo simulations using synthetic data. We show that the proposed estimator offers the lowest root-mean-square error (RMSE) at low SNR situations for a wide range of spectral widths. Finally, we evaluate the MPP algorithm performance using real data measured by RMA Argentinian weather radar. The results of tests performed are consistent with those of Monte-Carlo simulations and validate the proposed method.**

***Index Terms*—Doppler velocity estimation, Doppler weather radar, signal processing, spectral analysis.**

I. Introduction

Spectral moments estimation is one of the main objectives in weather radar signal processing, since these are closely linked to the characteristics of the observed meteorological targets. In particular, the first order moment normalized with respect to the zeroth moment is related to the mean radial motion of the scatterers present in the radar resolution volume and it is commonly called *mean velocity*, v_m, or *mean frequency*, f_m, both related by a simple change of scale [1].

There are a wide variety of proposed mean velocity estimators [2]–[12]. One of the simplest is the *Spectral Processing* (SP), which consists in the evaluation of the mean frequency, by definition, once the signal spectrum has been estimated. The Fast-Fourier Transform (FFT) makes this approach attractive due to its low computational load. However, the SP estimator is biased as a consequence of the finite FFT resolution [2].

Pulse-Pair Processing (PPP) is, probably, the most common approach to estimate the mean velocity. The PPP velocity estimator is proportional to the argument of the first autocorrelation lag estimate, $\hat{R}(T_s)$, being T_s the pulse repetition time (PRT), where $\hat{R}(T_s)$ is computed from contiguous pulse-pairs. This approach also has a low computational load, but its performance degrades significantly at low signal-to-noise ratios (SNR), below 10 dB, and when meteorological target spectral width increases [3].

There are alternatives that combine autocorrelation estimates at different lags, $\hat{R}(kT_s)$, $k \in \mathbb{N}$, in order to improve PPP performance. Two approaches are the *Poly-PPP* and the *Periodogram Maximization* estimators [2]. However, none achieves a consistent better performance than PPP [2]. Unlike PPP, which uses only partial autocorrelation information, these methods utilize the complete information contained in the autocorrelation but suffer from the drawback that the autocorrelation estimates for higher lags are poor.

The *Band Limited* (BL) estimator proposed in [5] can be viewed as a weighted sum of the $\hat{R}(kT_s)$, where the weights are the impulse response coefficients of the interpolation filter. The BL estimator outperforms PPP when the spectrum is asymmetric or when it has a medium to large spectral width. The *Multi-Lag Estimator* also uses the available autocorrelation estimates at multiple lags to fit a Gaussian function in order to estimate spectral moments and polarimetric parameters [6].

On the other hand, the methods based on optimal estimation criteria such as *Maximum Likelihood* [7] and subspace-based methods [8] can reach a very good performance, but their high computational cost excludes them from real-time applications. Finally, *Adaptive Filtering* techniques have been also proposed for Doppler spectral moment estimation. Based on a first order complex autoregressive series as the signal model, in [9] the authors deduce an optimal adaptive filter in terms of maximum a posteriori probability. However, its performance degrades significantly when the number of data samples is small and in a practical situation, where having more than 64 samples is uncommon, it is not recommended.

In practice, weather radars suffer from range ambiguity when short PRT is used to increase the unambiguous Doppler interval. Staggered-PRT techniques enable increasing the unambiguous velocity without degrading the unambiguous range [13]. Although there are different PRTs combinations [14], a two-PRT system is often used, where the pulse interval alternates between PRTs T_1 and T_2. The unambiguous velocity for this scheme depends on $T_u = T_2 - T_1$ and it is shown that as the ratio $\kappa = T_1/T_2$ is closer to one, the velocity estimation error increases [10]. For this reason, the use of $T_1 = 2T_u$ and $T_2 = 3T_u$ is often the chosen solution to this trade-off.

This work was supported by Universidad Nacional de Cuyo (UNCuyo) C038 4142/19, FONCYT PICT-2018-01277, Consejo Nacional de Investigaciones Científicas y Técnicas (CONICET), Universidad Nacional de Río Negro and Comisión Nacional de Energía Atómica (CNEA).

J. P. Pascual (juanpablo.pascual@ib.edu.ar), is with CONICET and Instituto Balseiro - Universidad Nacional de Cuyo. Argentina.

J. Cogo (jcogo@unrn.edu.ar), is with Universidad Nacional de Río Negro. Argentina.

A. Collado Rosell (arturo.collado@ib.edu.ar) is with CNEA. Argentina.

J. Areta (jareta@unrn.edu.ar) is with Universidad Nacional de Río Negro and CONICET. Argentina.

Manuscript received -.

A PPP extension for the staggered strategy (SPPP) is proposed in [10], where the mean velocity estimator is proportional to the argument difference of $\hat{R}(T_1)$ and $\hat{R}(T_2)$. It works on the whole unambiguous range but since it is computed as two estimators subtraction, in general, its variance is high.

In the *Magnitude Deconvolution* (MD) method [11] the staggered-PRT sequence is interpreted as a sequence uniformly sampled at T_u, that has zeros in the missing samples. The Fourier transform of the resulting sequence has replicas of the signal spectrum in some fractions of the Nyquist interval, whose number and positions depends on κ. When the spectrum is narrow enough that these replicas do not overlap, the MD strategy allows to reconstruct the original spectrum magnitude from which $\hat{R}(T_u)$ can be obtained. Hence, the mean velocity is computed using PPP through $\hat{R}(T_u)$. This method gives reasonably good velocity estimates even if the spectra are slightly wider and the replicas slightly overlap.

Finally, the *Dealising Method* (DA) [12] computes two PPP estimates $\hat{v}_1$ from $\hat{R}(T_1)$ and $\hat{v}_2$ from $\hat{R}(T_2)$. Since $T_2 > T_1 > T_u$ their respective unambiguous velocities follow $v_{a2} < v_{a1} < v_a$ and therefore $\hat{v}_1$ and $\hat{v}_2$ could be aliased. Admitting one-time aliases, only v_1 and $(v_1 \pm v_{a1})$ may belong to $(-v_a, v_a)$. In the same way, only v_2 and $(v_2 \pm v_{a2})$ may belong to $(-v_a, v_a)$. There is only one value that is common to both sets, and this is the right velocity estimate. Since $T_1 < T_2$ the variance of $\hat{v}_1$ is lower than the variance of $\hat{v}_2$. Thus, $\hat{v}_2$ is used only to decide between the values $\hat{v}_1$, $\hat{v}_1 - v_{a1}$ or $\hat{v}_1 + v_{a1}$, and this is the final output of the method. DA is slightly more complex than SPPP, however gives more accurate velocity estimates than the former staggered-PRT velocity estimators for a wide range of spectral widths.

In this paper we present an algorithm termed *Multi-Pulse Processing* (MPP) for spectrum mean frequency estimation in weather radar applications. MPP uses the complete information contained in the radar signal autocorrelation. It is based on a zero-finding of a functional that depends on multiple autocorrelation lags. To select the proper zero an initial estimate is required. Therefore MPP can be considered as an estimation refinement stage. The rest of the paper is organised as follows. In Section II, we introduce the problem statement and in Section III we derive the MPP algorithm steps. While MPP can be used for both uniform and staggered PRT sequences, we focus the analysis in staggered-PRT operation. We present numerical simulations results in Section IV including a performance comparison with the methods SPPP, MD and DA, in different SNR situations. In Section V MPP, SPPP and DA algorithms are tested on weather radar data to evaluate their performance in a real situation. Finally, we present conclusions in Section VI.

II. Problem Formulation

The Wiener-Khinchin theorem states that the autocorrelation function of a random process at lag T_s, $R(T_s)$, can be written in terms of its power spectral density (PSD), $S(f)$, through the inverse Fourier transform [15]

$$R(T_s) = \int_{-1/2T_s}^{1/2T_s} S(f) e^{j2\pi f T_s} df, \tag{1}$$

where T_s is the sample time interval, or the PRT in Doppler weather radar.

PPP assumes that the Doppler spectrum $S(f)$ consists only of a single peak due to backscatter from a weather phenomenon and it is symmetric with respect to the mean frequency f_m [1]. Then if we express (1) as

$$R(T_s) = e^{j2\pi f_m T_s} \int_{-1/2T_s}^{1/2T_s} S(f) e^{j2\pi (f - f_m) T_s} df, \tag{2}$$

the integral is real and f_m can be determined from the argument, $2\pi f_m T_s$, of $R(T_s)$. This is owing to the fact that the imaginary part of the integral in (2) is zero, i.e.

$$\int_{-1/2T_s}^{1/2T_s} S(f) \sin(2\pi (f - f_m) T_s) df = 0. \tag{3}$$

However, under the hypothesis that $S(f)$ is symmetric with respect to its mean frequency, the condition (3) is satisfied by any function $G(f)$, odd and periodic with period $1/T_s$, not only by $\sin(2\pi f T_s)$. Then, it is possible to define the functional

$$J(f_d) = \int_{-1/2T_s}^{1/2T_s} S(f) G(f - f_d) df, \tag{4}$$

that allows to calculate f_m such that $J(f_m) = 0$.

III. Algorithm

Since $G(f)$ is a periodic function, it can be written in terms of its Fourier series [16]

$$G(f) = \sum_{k=-\infty}^{\infty} g_k e^{j2\pi k f T_s}, \tag{5}$$

where g_k are the Fourier coefficients.

Replacing the expression (5) of $G(f)$ in (4) it is possible to rewrite the functional as

$$J(f_d) = \sum_{k=-\infty}^{\infty} g_k R(kT_s) e^{-j2\pi k f_d T_s}. \tag{6}$$

Although (6) is equivalent to (4), it is a more convenient form to solve the problem. Its time domain formulation avoids evaluation of the integral and computation of the PSD, allowing its application to any PRT strategy.

Then, the proposed MPP algorithm to estimate f_m consists in zero-finding of the real function $J(f_d)$ expressed in (6).

A. Practical Aspects

In practice, we have estimates of the autocorrelation function at a finite number of lags, $\hat{R}(kT_s)$ for $k = -K, ..., 0, ..., K$. Then the spectrum mean frequency estimate, $\hat{f}_m$, is obtained from

$$J(\hat{f}_m) = \sum_{k=-K}^{K} g_k \hat{R}(kT_s) e^{-j2\pi k \hat{f}_m T_s} = 0. \tag{7}$$

The problem defined by (7) does not have analytical solution and must be solved numerically [17].

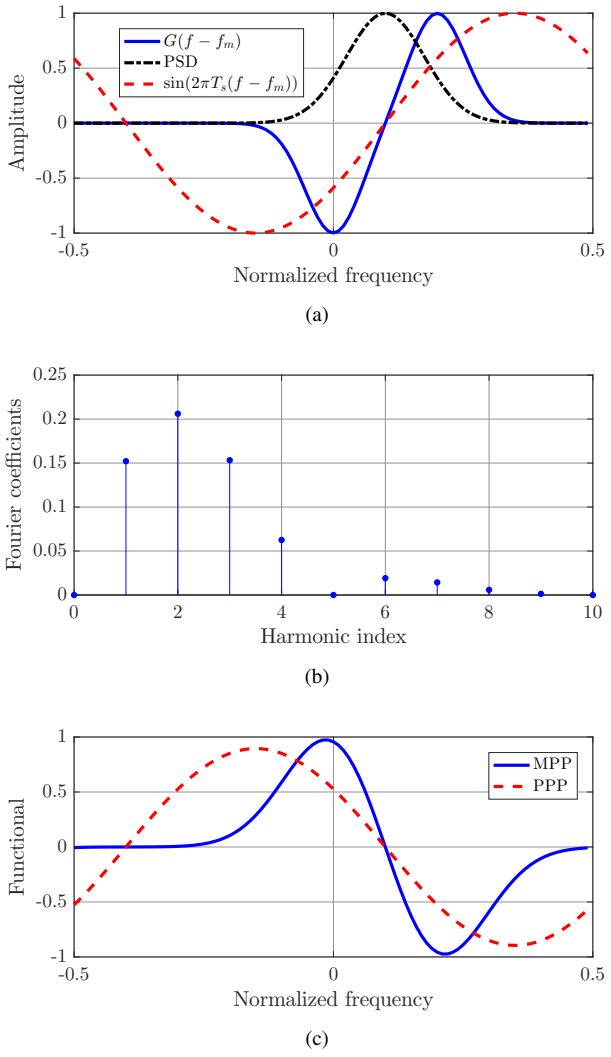

Figure 1. (a) Test functions. (b) Fourier coefficients of the MPP test function. (c) Functionals.

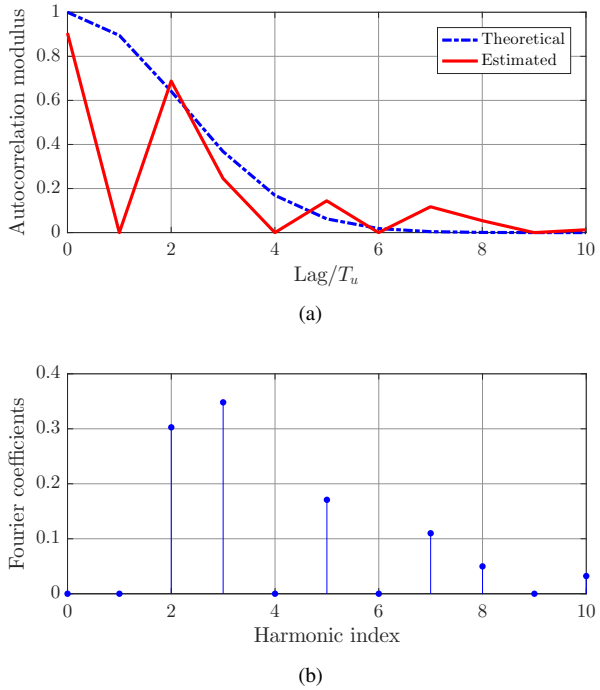

Figure 2. MPP for Staggered-PRT Sequences. (a) Autocorrelation. (b) Test function Fourier coefficients.

B. Choice of Test Function $G(f)$

The algorithm depends on the value of the coefficients g_k, which are determined by the shape of the test function $G(f)$. To our knowledge, there is not a unique optimal test function for all meteorological targets. However, we observe that there are some characteristics of the test function that improve the estimate accuracy.

Fig. 1(a) shows an example of a test function $G(f)$ together with the PPP test function, i.e. $\sin(2\pi(f-f_m)T_s)$, and a PSD, $S(f)$, that represents a weather target with mean frequency $0.1f_s$ and spectrum width $0.075f_s$, where $f_s = 1/T_s$. Note that if the support of $G(f)$ is similar to the support of $S(f)$, then the functional zero depends only on the weather spectrum. It reduces the mean velocity estimation error when there are other signals added to the weather component, like noise or ground clutter. However, to take advantage of this fact, a priori knowledge of the spectrum width is required.

In Fig. 1(b) we present the Fourier coefficients of this test function example. It should be noted that the autocorrelation estimation error increases as the lags kT_s increase and this error depends on the number of pulses in each coherent processing interval (CPI). In weather radar it is common to define the CPI as the number of pulses included in the antenna beam-width which for our datasets varies between 32 and 64 pulses. Then, considering beyond 6 or 7 autocorrelation lags the error is significant and also the autocorrelation for a typical meteorological target tends to zero, as can be seen in Fig. 2(a). Since the Fourier coefficients of the test function weight the autocorrelation estimates, $\hat{R}(kT_s)$, in the MPP functional (7), it is desirable to avoid high values of g_k for large k, i.e. it is recommended that $G(f)$ does not have fast variations. The number of coefficients must be also sufficient to correctly represent the test function. Then, for the test functions presented along the work, we have chosen the use of 10 coefficients as a balance between these conditioning factors. Finally, Fig. 1(c) shows the MPP and the PPP functionals computed from $G(f-f_m)$ and $\sin(2\pi(f-f_m)T_s)$, respectively.

C. Staggered-PRT Sequences

Without loss of generality, we restrict our analysis to a two-PRT system with $\kappa = T_1/T_2 = 2/3$. It is possible to construct an equivalent uniform sequence with PRT T_u, such that $T_1 = 2T_u$ and $T_2 = 3T_u$, where zero values are assigned to the missing samples.

Fig. 2(a) shows the theoretical autocorrelation modulus for a weather target with mean frequency $0.2f_s$, spectrum width $0.075f_s$ and power 1 [AU], where $f_s = 1/T_u$, together with an estimate of this autocorrelation computed using a 64-samples simulated staggered random sequence, with $\kappa = 2/3$ [18].

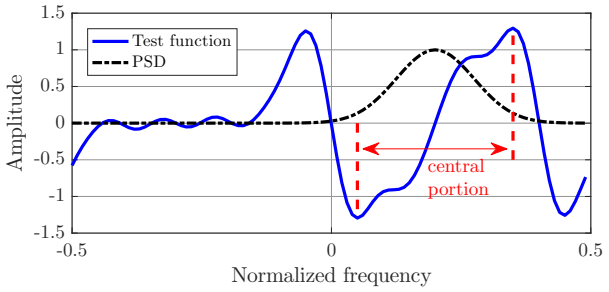

(a)

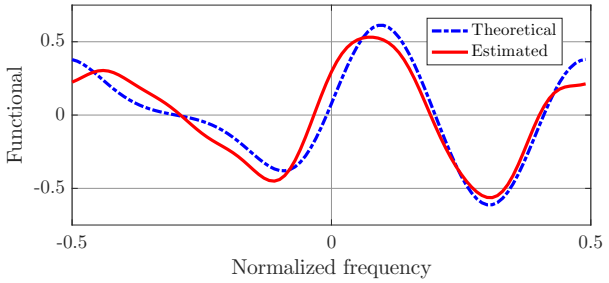

(b)

Figure 3. MPP for Staggered-PRT Sequences. (a) Test function. (b) Functional.

The zero values of the autocorrelation estimate at lags T_u, $4T_u$, $6T_u$ and $9T_u$ correspond to missing lags. Forcing the Fourier coefficients to be zero in the design of the test function, it is possible to control which autocorrelation lags do not contribute to the functional (7). We can then design the test function so that the g_k are zero for these missing lags, such as shown in Fig. 2(b).

Fig. 3(a) shows the test function corresponding to the Fourier coefficients of Fig. 2(b). Note that it has two positive peaks and two negative peaks. This unwanted behaviour is due to the null in the fundamental harmonic and it produces additional zeros that do not correspond to weather target mean frequency. In Fig. 3(b) the theoretical and estimated functionals for the staggered-PRT sequences are shown. The functional estimate is computed using the autocorrelation estimate presented in Fig. 2(a). Note that only the zero at $0.2f_s$ is valid, the others are consequence of the test function shape. Hence, it is not enough to find the zeros of the functional to determine the mean velocity estimate, the algorithm requires a procedure to choose the right zero.

D. Function Design for Staggered-PRT

The test function design is important for the MPP algorithm. It depends on the weather radar operation strategy and it would be interesting to study the optimum function design subject to the radar return signal composition. For the test function, $G(f)$, used throughout the work, we propose to combine three basic periodic functions, with period $1/T_u$, $G_a(f)$, $G_b(f)$ and $G_c(f)$, such that $G(f) = G_a(f) + G_b(f) + G_c(f)$ results also

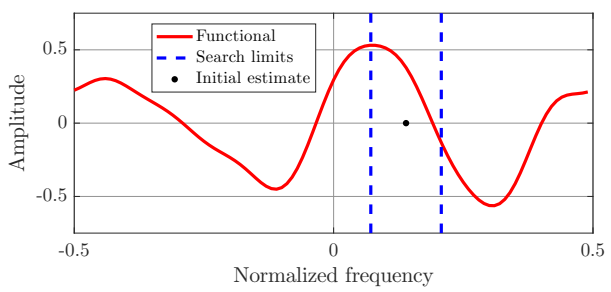

Figure 4. MPP algorithm procedure.

a periodic function with period $1/T_u$. We propose defining

$$G_{a1}(f) = A_a \sin(2\pi f T_a) \qquad -0.5/T_a < f \leqslant 0.5/T_a, \quad (8)$$

$$G_{b1}(f) = \frac{A_b}{\sqrt{2\pi}\sigma_b}\left[e^{-\frac{(f+\mu_b)^2}{2\sigma_b^2}} - e^{-\frac{(f-\mu_b)^2}{2\sigma_b^2}}\right], \quad (9)$$

$$G_{c1}(f) = A_c\left[\text{sinc}^2\left(\frac{f-\mu_c}{\sigma_c}\right) - \text{sinc}^2\left(\frac{f+\mu_c}{\sigma_c}\right)\right], \quad (10)$$

where $G_{a1}(f)$, $G_{b1}(f)$ and $G_{c1}(f)$ are the central periods of the functions $G_a(f)$, $G_b(f)$ and $G_c(f)$, respectively. The choice of these functions is not unique and it is based on having sufficient degrees of freedom to force to zero the Fourier coefficients g_k for the missing lags when a staggered-PRT with $\kappa = 2/3$ is used. Then, the parameters of the functions, A_a, T_a, A_b, μ_b, σ_b, A_c, μ_c and σ_c, are chosen to zero the Fourier coefficients that multiply the missing lags of the autocorrelation function. Thus, considering the first ten lags, for $\kappa = 2/3$ the conditions to compute the parameters are $g_k = a_k + b_k + c_k = 0$, for $k = 1, 4, 6, 9$, being g_k, a_k, b_k and c_k the Fourier coefficients of $G(f)$, $G_a(f)$, $G_b(f)$, and $G_c(f)$, respectively. The values of the test function parameters that satisfy the required conditions are the following: $A_a = 1$, $T_a/T_u = 3$; $A_b T_u = -1/12$, $\mu_b T_u = 1/6$, $\sigma_b T_u = 1/40$; $A_c = -6/5$, $\mu_c T_u = 1/4$ and $\sigma_c T_u = 3/25$.

E. Multi-Pulse Processing Steps

The functional ambiguity depends on the test function, so it can also occur for uniform-PRT sequences. To deal with this issue, we propose to search the true zero around an initial estimate obtained through a primary method, e.g. PPP.

In summary, the steps of the MPP algorithm are:

1) Define a test function and evaluate its first K Fourier coefficients, g_k.
2) Estimate K lags of the autocorrelation, $\hat{R}(kT_s)$.
3) Compute the functional $J(f_d)$.
4) Evaluate an estimate of the mean frequency $\hat{f}_0$ by means of a primary method.
5) Define the initial zero search interval as 40% of the test function *central portion*, around the initial estimate $\hat{f}_0$.
6) Verify that the functional at the interval lowest and highest frequencies is positive and negative, respectively.
7) If the condition of step 6) is satisfied, search the functional zero in the defined interval and accept the result as the mean frequency estimate $\hat{f}_m$.

8) If the condition of step 6) is not satisfied, increase the interval, maximum six times, in steps of 5% of the function *central portion* until the condition of step 6) is satisfied. If the condition of step 6) is satisfied, do step 7). Otherwise, do nothing and accept the initial estimate as the mean frequency estimate $\hat{f}_m$.

In Fig. 4 the steps 4) to 6) are schematically represented. We define the *central portion* of the test function as the interval between the central negative and positive peaks, as can be seen in Fig. 3(a). Note that the condition of the step 6) applies when the function within the *central portion* is increasing. If it is decreasing, the condition should be inverted. It is important to remark that as usual in any numerical method [17] there is not a unique way to define the zero search interval. We choose to limit the search interval to a fraction of the test function *central portion* defined as above to prevent as much as possible including a non-correct zero, i.e. generated by the shape of the test function.

IV. Numerical Simulations

A series of Monte-Carlo simulations has been conducted in order to verify the correct operation of the algorithm and to compare its performance with other mean velocity estimation methods. While MPP can be used for uniform-PRT, we focus the analysis in staggered-PRT operation. For the case of uniform-PRT and the proposed test functions MPP presents a performance similar to PPP.

A 10-cm wavelength radar is assumed, with a basic sampling period of $T_u = 0.5$ ms and a ratio $\kappa = 2/3$, which gives the staggered PRTs $T_1 = 1$ ms and $T_2 = 1.5$ ms. The signal model consists of a Gaussian random sequence composed of a Gaussian-shaped PSD meteorological target plus white noise [18]. We have performed studies that involve computing the statistic of errors and execution times, varying the primary method, the SNR and the spectral width. For each setting of these parameters we have generated 10000 different runs of 64-samples length data records. In all situations the MPP algorithm uses the test function derived in Section III-D and Newton's method for zero-finding [17]. We have set the zero-finding tolerance to 10^{-7} as a good balance between the expected number of iterations and the estimate error. With this value we observe that on average the number of iterations has been between 3 and 4 for every primary method, every SNR and every spectral width tested.

In addition to the MPP algorithm, we have tested the pulse-pair processing method for staggered sequences (SPPP) [10]; the velocity estimation using magnitude deconvolution (MD) [11]; and the velocity estimation from $\hat{R}(T_1)$ and dealiasing from both $\hat{R}(T_1)$ and $\hat{R}(T_2)$ (DA) [12].

Fig. 5(a) shows the estimation root-mean-square error (RMSE) of the estimates for each method, as a function of the SNR for 4 m/s of spectrum width. The result and the spectrum width are presented in velocity terms, making use of the relation $v = -\lambda f/2$, being λ the wavelength, v the Doppler velocity and f the Doppler frequency. For comparison we have included the exact Cramér-Rao bound (CRB) obtained for the signal model used [19]. The MPP algorithm is presented using

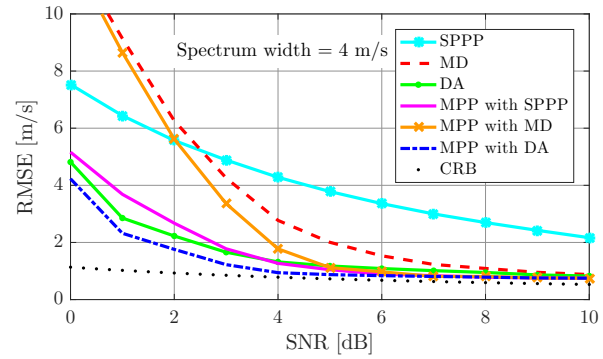

(a)

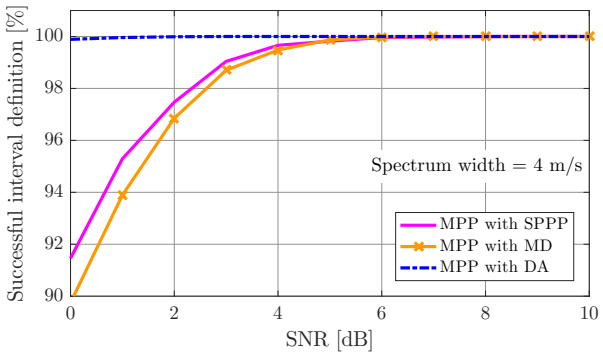

(b)

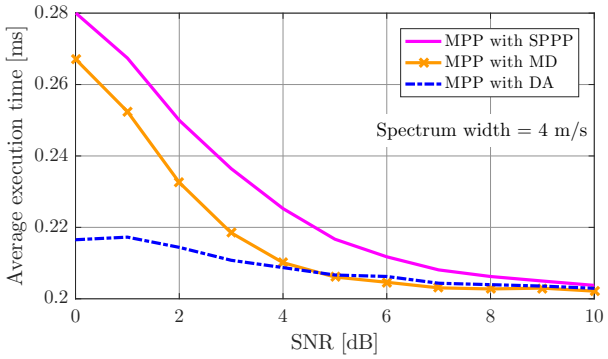

(c)

Figure 5. (a) Velocity estimation RMSE. (b) Percentage of interval definition successfully. (c) Average execution time.

SPPP, MD and DA as the primary methods to obtain the initial estimate in step 4) (these will be referred as MPP with SPPP, MD or DA, respectively).

Although the estimation biases are not plotted, it is important to mention that these biases are very small relative to the corresponding RMSE and the CRB. They are below the 5% of the CRB for most SNR values and below 10% of the CRB for all the SNR values. From a practical point of view all the estimators can be considered unbiased.

Fig. 5(a) shows that the SPPP estimator presents on average the worst performance of all methods, with its RMSE far from the CRB across the range of analyzed SNR values. As explained in [12] this is a consequence of the fact that

the SPPP result involves the difference in phases of two lag autocorrelation estimates. The MD estimator shows the worst performance for SNR values below 3 dB, attributable to the increased influence of noise due to the spillover of its power spectrum caused by non-uniform sampling aliases. However, its RMSE decreases faster than that of SPPP as the SNR increases and it is close to the CRB at a 10 dB of SNR. As expected, the DA estimator shows a better performance than SPPP and MD and its RMSE approximates the CRB faster than these methods.

Regarding MPP, it always improves the performance of the corresponding primary method. However, the performance achieved depends on the primary method used, being MPP with DA the estimator with lowest RMSE and closest to CRB, in the analyzed SNR range. It is interesting to note that for SNR values above 3 dB the RMSE of MPP with SPPP is lower than the RMSE of DA and MPP with MD presents the same behaviour for SNR values above 5 dB. This shows that MPP achieves a significant improvement for a wide SNR range even when the primary estimate is poor.

MPP algorithm defines a search interval and checks that a zero is contained on this interval. If this process fails, then MPP returns the primary estimate. Fig. 5(b) shows the percentage of times that the interval definition is successful for each primary method. Note that the results are directly related to the quality of the primary estimate. For SNR of 0 dB MPP with DA defines a search interval the 99.89% of the runs and for SNR of 3 dB or larger the 100% of the runs. Instead, MPP with SPPP and MPP with MD define a search interval the 91.46% and 89.75% of the runs, respectively, for 0 dB of SNR and they reach 100% for 7 dB of SNR. This behaviour explains why in Fig. 5(a) the MD and MPP with MD RMSE curves are close for low SNR. Inaccurate primary estimates prevent to define a search interval and they have a great influence in the average errors of both methods.

As the MPP algorithm is iterative, the exact calculation of the number of operations required is difficult to find. To give a complexity notion we have evaluated the average runtime for all the methods using the same platform, a PC with Intel Core i7-3770 (3.4 GHz $\times$ 4) processor and 16 GB of RAM. In Fig. 5(c) the 64–samples CPI average execution times for MPP using the different primary methods are presented. These values do not take into account the time required to obtain the primary estimate. MD, DA and SPPP are not iterative, thus their execution times do not depend on SNR and their average execution times are 0.13 ms, 0.05 ms and 0.03 ms, respectively. Then, in situations of medium or low SNR, MPP can provide a significant improvement in velocity estimation performance, with an increase in computational load. In these situations its use is recommended. Although the increase in computational load is not prohibitive, its use in high SNR situations may not be justified in practical terms.

Fig. 6 shows the RMSE of the estimates for each method and the CRB, as a function of the spectrum width, for SNR of 5 dB and 15 dB. In this case, the MPP algorithm uses only DA as the primary method because in the previous analysis it presented the best performance. Again, biases are not plotted, but it is important to mention that they are low for all methods.

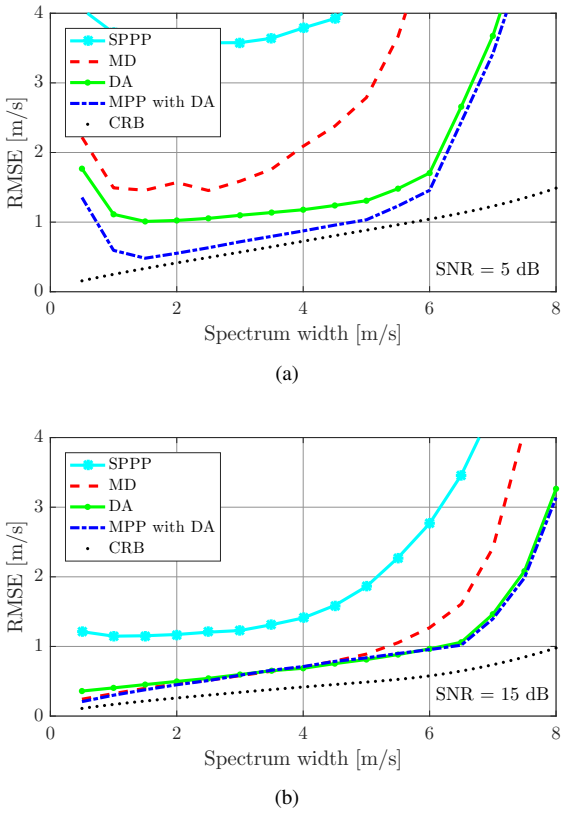

Figure 6. Velocity estimation RMSE. (a) SNR of 5 dB. (b) SNR of 15 dB.

In the spectral width range from 1 to 7 m/s, the biases of MPP and DA are below 5% of the CRB and the biases of SPPP and MD are below 10% of the CRB.

The SPPP estimator has the largest RMSE in the tested situations. While the MD estimator presents a good performance for an SNR of 15 dB and spectrum widths below 5 m/s, for an SNR of 5 dB its performance is not good for any spectrum width.

Finally, MPP and DA present the best performance among the analyzed methods. For a 15 dB SNR, the performance of both methods are similar, with MPP being slightly better than DA for narrow spectral widths. However, for a 5 dB SNR, the improvement in performance obtained using MPP with respect to using DA becomes appreciable. Note that the DA RMSE moves away from the CRB while the MPP RMSE is close to the CRB for spectrum widths between 1 m/s and 6 m/s.

V. Testing on Real Weather Radar Data

In this section, the MPP algorithm is tested on real weather radar data to evaluate its performance in a realistic scenario. The measurements were collected by the RMA-12 Argentinian weather radar, located in San Carlos de Bariloche city. RMA-12 is a C-band polarimetric radar, designed and developed by INVAP. Specifically, the data were recorded on August 18, 2018, under intense rain meteorological conditions. The shown results correspond to a complete sweep of the horizontal polarization (HH), using a staggered-PRT with $\kappa = 2/3$ and an unambiguous velocity of 25 m/s, at 7.2 degrees elevation

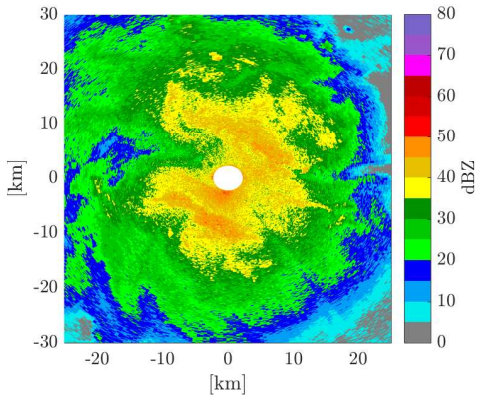

Figure 7. Reflectivity of the real weather radar data.

angle, ensuring that there were no ground clutter components present. Fig. 7 shows the reflectivity plan position indicator (PPI) of the data.

Figs. 8(a), 8(b) and 8(c) show the PPI displays of the Doppler velocity estimation obtained from the data set with the SPPP, DA and MPP methods, respectively. The MPP algorithm uses DA as the primary estimate. In all of the PPI displays a central zone can be recognized, where the velocity changes are smooth. This zone corresponds to a storm. In the corners (especially on the right side) the velocity values present a random behaviour. This second zone corresponds mainly to noise, without the presence of any appreciable weather signal component. Note, that the described behaviour is consistent with the reflectivity data presented in Fig. 7.

In the storm zone, an approximately vertical center strip of zero-velocity (in gray tone) is observed, to the right of which the velocity is positive and increases in magnitude (dark red tones to light red tones) as the azimuth tends to $90°$, while to the left of the strip the velocity is negative and increases in magnitude (dark green tones to light green tones) as the azimuth tends to $-90°$. The foregoing can be interpreted as the storm moving above the radar in approximately west-to-east direction, where the changes in magnitude as the azimuth varies correspond to the projection of the wind speed in the direction of observation.

Note from Fig. 8(a) that the SPPP estimates present more dispersion than the estimates obtained with the other methods. Graphically, this effect appears as less defined edges between regions of different velocity. While it occurs throughout the PPI display, this can be seen clearly in the central vertical strip in gray, where there is a greater color contrast.

On the other hand, DA and MPP estimates, Figs. 8(b) and 8(c), show a similar behaviour. We evaluated the root-mean-square (RMS) of the Difference of Velocity Estimates (DVE) between DA and MPP and the RMS of DVE between SPPP and MPP, obtaining 0.31 m/s and 2.29 m/s, respectively, which quantitatively supports the former qualitative description. These results are consistent with the Section IV discussion, considering that even at ranges larger than 25 km, the SNR is over 15 dB.

Due to the high SNR the DA and MPP methods present a comparable performance. Given their theoretical performance, it is useful to study their operation under adverse SNR conditions. Since we do not have real radar datasets in this situation, we artificially modified the available dataset in order to degrade the SNR. The procedure steps are described below.

First, we estimate the noise power using radar range resolution volumes that do not contain weather signal components (mainly outside the ranges shown in Fig. 7) [20]. Then, we estimate the SNR of each coherent processing interval (CPI) in the storm zone. Assuming that the signal and the noise are independent, we subtract the noise power to the total signal power, and we divide the result by the noise power to obtain the SNR estimate. Finally, in those CPI where the SNR is greater than 5 dB we add synthetic noise with circularly-symmetric normal distribution, whose variance is such that the SNR of the resulting signal is 5 dB.

Using the modified dataset, that we call *noisy*, we estimate the Doppler velocity by means of SPPP, DA and MPP. The results are presented in Figs. 8(d), 8(e) and 8(f), respectively.

Note that the SPPP estimates present a great degradation when the noisy dataset is used. The PPI display of Fig. 8(d) has even less defined edges between regions of different velocity than Fig. 8(a). The degradation is moderate for the DA estimates, Figs. 8(b) and 8(e), while it is practically indistinguishable for the MPP estimates, Figs. 8(c) and 8(f).

To observe the noise degradation on DA and MPP velocity estimates Figs. 9(a) and 9(b) show the DVE of DA before and after noise addition (difference between Figs. 8(e) and 8(b)) and the DVE of MPP before and after noise addition (difference of Figs. 8(f) and 8(c)), respectively. The white zone of these figures corresponds to those CPIs where the original data consists mainly of noise, i.e. those CPIs in which the estimated SNR is lower than 5 dB and synthetic noise has not been added.

These figures allow to notice the improved performance of MPP over DA for low SNR. Note that at the center of the PPI displays of Figs. 9(a) and 9(b) the differences are remarkable. However, around the outer edges of the analyzed region it is observed that both methods have a similar performance. We conjecture that there are two possible reasons for this behaviour. Since the SNR of the original signal is low in this region (the SNR decreases with the range, because the echo power decreases with the range while the noise power remains almost constant) the estimates obtained there before the noise addition already have high variance, which increases the variance of the subtraction. In addition, the low SNR impacts on the signal power estimation and it causes that the final SNR, after the addition of noise, might be lower than the intended 5 dB.

For a quantitative analysis of the results, we will consider only those CPIs in which the original SNR is greater than 15 dB which ensures reliable estimates. In these CPIs we can assume, based on the results of Section IV, that both DA and MPP estimates over the original dataset will take similar values. Since we are processing observational data for which the true values are unknown, we consider the high SNR estimates as a good approximation to the *ground truth*. It is important to note that 84% of the CPIs to which noise was added (no-white regions of Figs. 9(a) and 9(b)) meet this

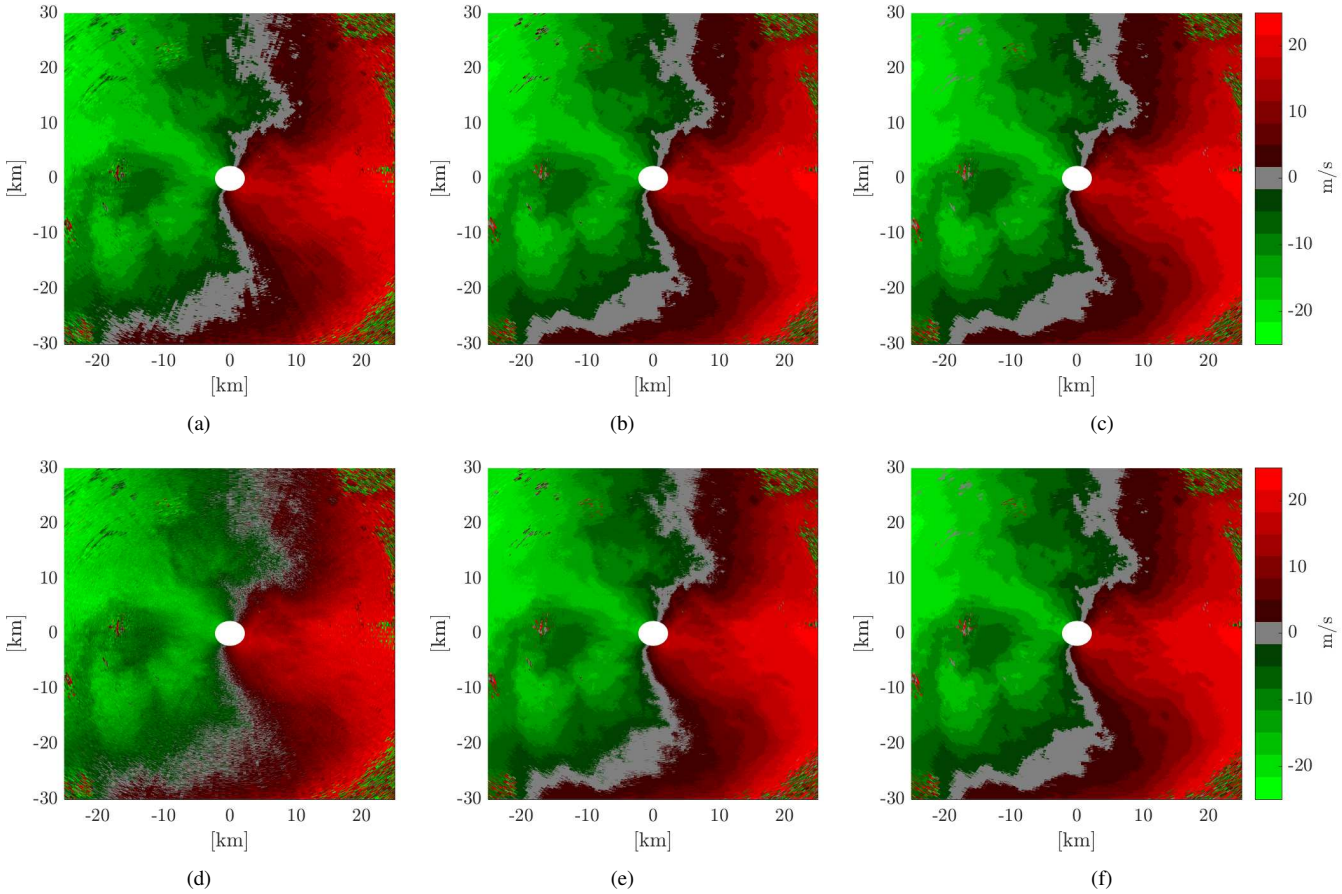

Figure 8. Doppler velocity estimation algorithms test on real weather radar data. (a) SPPP. (b) DA. (c) MPP with DA. (d) Noisy SPPP. (e) Noisy DA. (f) Noisy MPP with DA.

condition and will be included in the analysis.

The RMS of the DVE before and after noise addition (considering the CPIs that meet the previously discussed condition) is equal to 1.11 m/s for DA and 0.79 m/s for MPP, which quantitatively supports the previous qualitative analysis. Even when for the real dataset we do not have a reliable knowledge of the spectral width, the latter results are also consistent with the separation between the performance curves of both methods presented in Fig. 6(a).

To complete the analysis, Fig. 10 shows approximate probability density functions (PDF) of the DVEs, obtained by means of histograms. The green curve corresponds to the PDF of the DVE between DA and MPP before noise addition (i.e. difference of Figs. 8(b) and 8(c)). This is a narrow PDF concentrated around zero, which confirms that DA and MPP estimates show a similar behaviour for high SNR. The blue curve corresponds to the PDF of DVE of MPP before and after noise addition (i.e. Fig. 9(b)). This PDF is very similar to the previous one, which denotes that the MPP velocity estimates obtained for the noisy dataset have a similar error to the velocity estimates obtained with the same method for the original dataset. The black curve corresponds to the PDF of the DVE of DA before and after noise addition (i.e. Fig. 9(a)). This PDF is centered around zero, but has a greater dispersion than the previous PDFs. Then, unlike what happens with MPP, the velocity estimates obtained for the noisy dataset using DA have a greater error than those velocity estimates obtained using DA for the original dataset. As expected, these results are consistent with the analysis of Fig. 9. Finally, the red curve corresponds to the PDF of the DVE between DA and MPP after noise addition (i.e. difference of Figs. 8(e) and 8(f)). It is also a wide PDF centered around zero, which denotes a significant difference between DA and MPP estimates. The comparison of this PDF with the green PDF and with the blue PDF allows to appreciate the improvement of the MPP method over DA.

VI. Conclusion

In this paper we present the novel Multi-Pulse Processing algorithm for improving mean velocity estimation. Essentially, MPP consists of the numerical optimization of a functional, which is composed of data autocorrelation estimates at multiple lags. We introduce the theoretical formulation and we derive the algorithm steps. It is worth pointing out that MPP operates as a second Doppler velocity estimation stage, i.e. it needs a seed that has to be obtained by means of a primary method, which will be improved after applying MPP.

The method can be used for uniform-PRT sequences and staggered-PRT sequences. However, the analysis performed is focused on staggered-PRT sequences, because for uniform-PRT the method does not show improvement over PPP. This

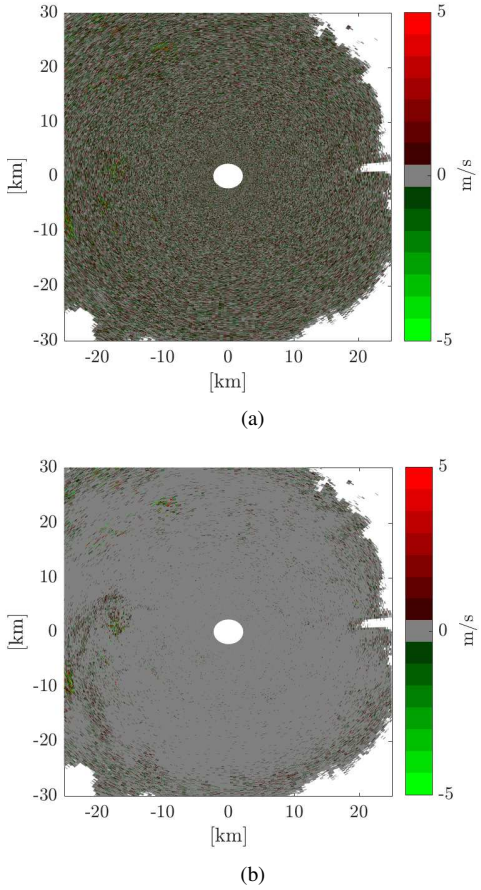

Figure 9. DVE before and after noise addition. (a) DA. (b) MPP with DA.

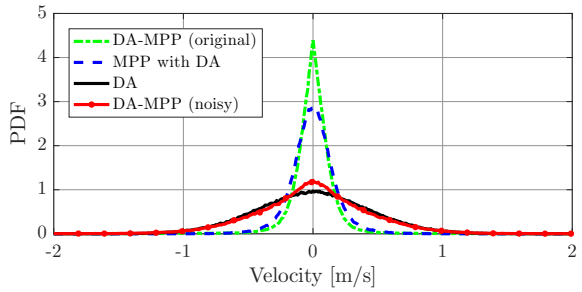

Figure 10. PDF estimates of the DVE.

is true for the set of test functions used, which consists of combinations of the kernels presented on Section III-D, for which no claim of optimality is done. The calculation of optimal test functions for uniform-PRT and staggered-PRT will be studied in the future. Note that we also restrict the analysis to the PRT ratio $\kappa = 2/3$ because it is the most widely used. If a different PRT ratio is used, the set of missing lags of the estimated autocorrelation will be different. Thus, for another value of κ, the parameters of the test function must be derived by forcing to zero the Fourier coefficients of the test function on the corresponding set of missing lags.

We evaluate the estimation bias and the RMSE versus SNR, by means of Monte-Carlo simulations, considering three well established primary methods of similar complexity: SPPP, MD and DA. We observed that MPP always improves the performance of the corresponding primary method over the entire range of tested SNR values. We also observed that in statistical terms, the quality of the initial estimate affects the MPP final performance, so it is recommended to choose the best available estimator for the first stage. For this reason, in the following analysis we present only the results of MPP with DA as the primary method.

Also, by means of Monte-Carlo simulations, we evaluate the estimation bias and RMSE versus spectral width, considering two representative values of SNR: 5 dB and 15 dB. We show that for 5 dB of SNR, MPP with DA presents a better performance than SPPP, MD and DA, i.e. the MPP RMSE is close to the CRB while the RMSE of the other methods move away from the CRB. On the other hand, for 15 dB of SNR, MPP has little room for improvement over the other methods, but still manages to give slightly better estimates. In this last situation, MPP has similar performance to MD and DA methods for a wide spectral width range, while SPPP presents the worst performance. Hence, from a practical viewpoint, the use of MPP is justified for low SNR as it implies an additional computational cost. In the simulations we assume 64 pulses, however if the number of input data samples increases, the autocorrelation estimation improves and, consequently, the error in the velocity estimates is reduced for all methods and especially for MPP.

Regarding bias, it is observed that their values remained below 10% (below 5% in most cases) of the respective CRB values, which allows us to say that the analyzed estimators are unbiased in practical terms.

We also compare the performance of the MPP estimator, using DA as primary estimate, with the SPPP and DA estimators using real weather radar data. We show that MPP and DA outperform SPPP, but MPP and DA have a similar performance because the SNR of the dataset is high. To study the performance at lower SNR, we add synthetic noise to the data, in order to get a 5 dB final SNR. In the case of the SPPP estimator, its performance degrades drastically. As expected, the MPP estimates present a lower dispersion than DA. Consistently with numerical simulation results, the MPP performance with the original dataset is similar to the MPP performance with the modified dataset, improving the DA primary estimates quality, especially, in the second situation. The greatest advantage of MPP is its performance in conditions of low weather data SNR.

The symmetric spectra assumption could be a limitation for all the methods used in this work. A possible next step is to study their performance when using them with asymmetrical spectral data. However, it is necessary to find a representative asymmetrical spectral model for meteorological targets. This may be accomplished using for example autoregressive series.

Finally, it might be of interest to investigate the test function design to reduce the velocity estimate ambiguity and also to mitigate the effect of residual clutter after filtering when it is present. Another future step is the study of test functions that could present some advantage in the estimation, e.g. desensitize the method with respect to the initial estimate.

ACKNOWLEDGMENT

The authors would like to thank Roberto Costantini for providing useful comments that helped to develop the work. RMA data was provided by Secretaría de Infraestructura y Política Hídrica, Ministerio del Interior, Obras Públicas y Vivienda of the Argentinean National Government framed within the Argentinean SINARAME Project.

REFERENCES

[1] R. J. Doviak and D. S. Zrnić, *Doppler Radar and Weather Observations, 2nd Ed.* San Diego Cal.: Academic Press, 1993.

[2] P. Mahapatra and D. Zrnić, "Practical algorithms for mean velocity estimation in pulse Doppler weather radars using a small number of samples," *IEEE Trans. Geosci. Remote Sens.*, vol. GE-21, no. 4, pp. 491–501, Oct. 1983.

[3] D. Zrnić, "Spectral moment estimates from correlated pulse pairs," *IEEE Trans. Aerosp. Electron. Syst.*, vol. AES-13, no. 4, pp. 344–354, Jul. 1977.

[4] ——, "Estimation of spectral moments for weather echoes," *IEEE Trans. Geosci. Remote Sens.*, vol. 17, no. 4, pp. 113–128, Oct. 1979.

[5] J. Dias and J. Leitão, "Nonparametric estimation of mean Doppler and spectral width," *IEEE Trans. Geosci. Remote Sens.*, vol. 38, no. 1, pp. 271–282, jan 2000.

[6] L. Lei, G. Zhang, R. Doviak, R. Palmer, B. Cheong, M. Xue, Q. Cao, and Y. Li, "Multilag correlation estimators for polarimetric radar measurements in the presence of noise," *J. Atmos. Oceanic Technol.*, vol. 29, pp. 772–795, Jun. 2012.

[7] E. Chornoboy, "Optimal mean velocity estimation for Doppler weather radars," *IEEE Trans. Geosci. Remote Sens.*, vol. 31, no. 3, pp. 575–586, May 1993.

[8] E. Boyer, P. Larzabal, C. Adnet, and M. Petitdidier, "Parametric spectral moments estimation for wind profiling radar," *IEEE Trans. Geosci. Remote Sens.*, vol. 41, no. 8, pp. 1859–1868, Aug. 2003.

[9] M. Pinsky, J. Figueras i Ventura, T. Otto, A. Sterkin, A. Khain, and H. Russchenberg, "Application of a simple adaptive estimator for an atmospheric Doppler radar," *IEEE Trans. Geosci. Remote Sens.*, vol. 49, no. 1, pp. 115–127, Jan. 2011.

[10] D. Zrnić and P. Mahapatra, "Two methods of ambiguity resolution in pulse Doppler weather radars," *IEEE Trans. Aerosp. Electron. Syst.*, vol. AES-21, no. 4, pp. 470–483, Jul. 1985.

[11] M. Sachidananda and D. S. Zrnić, "Clutter filtering and spectral moment estimation for Doppler weather radars using staggered pulse repetition time," *J. Atmos. Oceanic Technol.*, vol. 17, pp. 323–331, Mar. 2000.

[12] ——, "An improved clutter filtering and spectral moment estimation algorithm for staggered PRT sequences," *J. Atmos. Oceanic Technol.*, vol. 19, pp. 2009–2019, Dec. 2002.

[13] M. A. Richards, *Fundamentals of Radar Signal Processing*. New York: McGraw-Hill, 2005.

[14] M. Tahanout, A. Adane, and J. Parent du Châtelet, "An improved M-PRT technique for spectral analysis of weather radar observations," *IEEE Trans. Geosci. Remote Sens.*, vol. 53, no. 10, pp. 5572–5582, Oct. 2015.

[15] A. Papoulis, *Probability, Random Variables, and Stochastic Processes*, 3rd ed. New York: McGraw-Hill, 1991.

[16] A. V. Oppenheim, A. S. Willsky, and S. H. Nawad, *Signals and Systems*, 2nd ed. Upper Saddle River, NJ: Prentice Hall, 1997.

[17] E. Isaacson and H. B. Keller, *Analysis of Numerical Methods*. New York: Dover Publications, 1966.

[18] D. Zrnić, "Simulation of weatherlike Doppler spectra and signals," *J. Appl. Meteor.*, vol. 14, pp. 619–620, Jan. 1975.

[19] R. Frehlich, "Cramér-Rao bound for Gaussian random processes and applications to radar processing of atmospheric signals," *IEEE Trans. Geosci. Remote Sens.*, vol. 31, no. 6, pp. 1123–1131, Nov. 1993.

[20] I. Ivić, C. Curtis, and S. Torres, "Radial-based noise power estimation for weather radars," *J. Atmos. Oceanic Technol.*, vol. 30, p. 2737–2753, Dec. 2013.

Juan P. Pascual received his Eng. (2006) and Ph.D. (2014) degrees at the Universidad Nacional de La Plata (UNLP), Argentina. He worked in the design and FPGA implementation of control strategies for Electric Arc Furnaces in Tenaris (2008-2010). His postdoctoral experience include a research visit to the Instituto Balseiro in Bariloche (2015). He is currently a Professor at the Instituto Balseiro and a Researcher at the CONICET, Argentina. His research interests focus on statistical signal processing in radar and communication applications.

Jorge Cogo received his Eng. (2008) and M.Sc. (2016) degrees at the Universidad Nacional de La Plata (UNLP), Argentina. He worked on the design and implementation of GNSS receivers for space applications, mainly as a software engineer (2008–2017). He is currently a professor and researcher at the Universidad Nacional de Río Negro. His research interests focus on statistical signal processing in radar, communication and GNSS applications.

Arturo Collado Rosell was born in Havana, Cuba. He recieved a bachelor degree in Physics in 2015 and the MSc in Physics in 2016, both at the Balseiro Institute, Argentina. He is currently a Ph.D. candidate of the Balseiro Institute with a fellowship for postgraduate studies granted by the National Comision of Atomic Energy. His research interest are related to the digital signal processing, radars and machine learning.

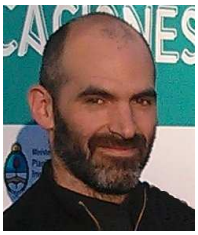

Javier Areta graduated as an Electronics Engineer from the National University of La Plata, Argentina, in 2001, and received the Ph.D. degree in Electrical Engineering from the University of Connecticut in 2008. He is an Associate Professor at the Department of the Electrical Engineering of the National University of Río Negro in Bariloche, Argentina. His research interests are in the area of statistical signal processing, particularly in radar applications.